Joint NICER/IXPE Workshop 2024

A NICER+NuSTAR view on the ultraluminous X-ray source NGC 4190 ULX1

Federico A. Fogantini

Instituto Argentino de Radioastronomía

July 31, 2024

Co-authors: J. Combi, E. Saavedra, F. García, L. Abaroa, G. Romero, N. Cruz-Sánchez, P. Luque Escamilla, J. Martí

DOI: 10.1051/0004-6361/202348895

I. Introduction to Ultraluminous X-ray sources (ULXs)

ULXs are X-ray binary systems with observed (apparent) luminosities exceeding the Eddington limit for stellar mass compact objects.

Main proposals to explain this phenomenon:

- Intermediate mass black holes (IMBH, 10^3- $10^5 M_\odot$) accreting at sub Eddington rates (same features as galactic XRBs).

- Stellar mass compact objects (BH, NS) accreting at supercritical rates from Roche filling companion, giving rise to accretion disk winds (forming funnels). (SS433, galactic example.)

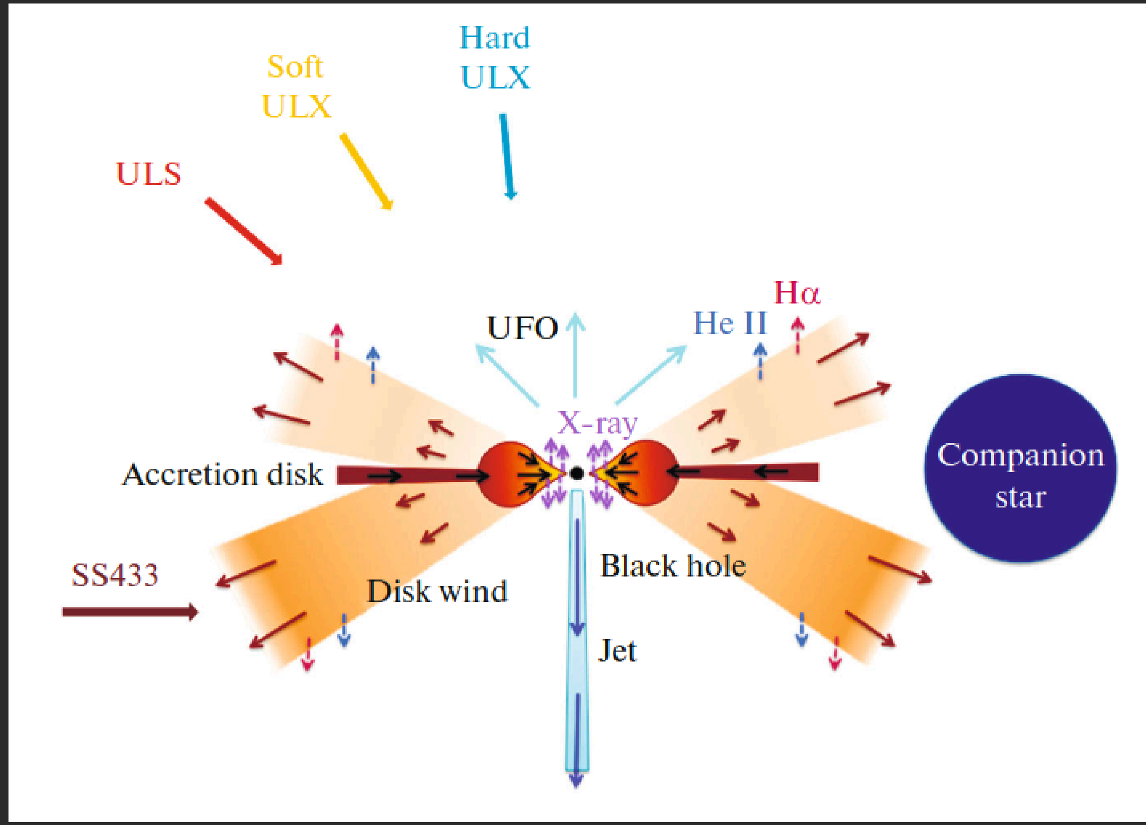

Fabrika et al. 2021

I. Introduction to Ultraluminous X-ray sources (ULXs)

ULXs are X-ray binary systems with observed (apparent) luminosities exceeding the Eddington limit for stellar mass compact objects.

Main proposals to explain this phenomenon:

- Intermediate mass black holes (IMBH, 10^3- $10^5 M_\odot$) accreting at sub Eddington rates (same features as galactic XRBs).
- Stellar mass compact objects (BH, NS) accreting at supercritical rates from Roche filling companion, giving rise to accretion disk winds (forming funnels). (SS433, galactic example.)

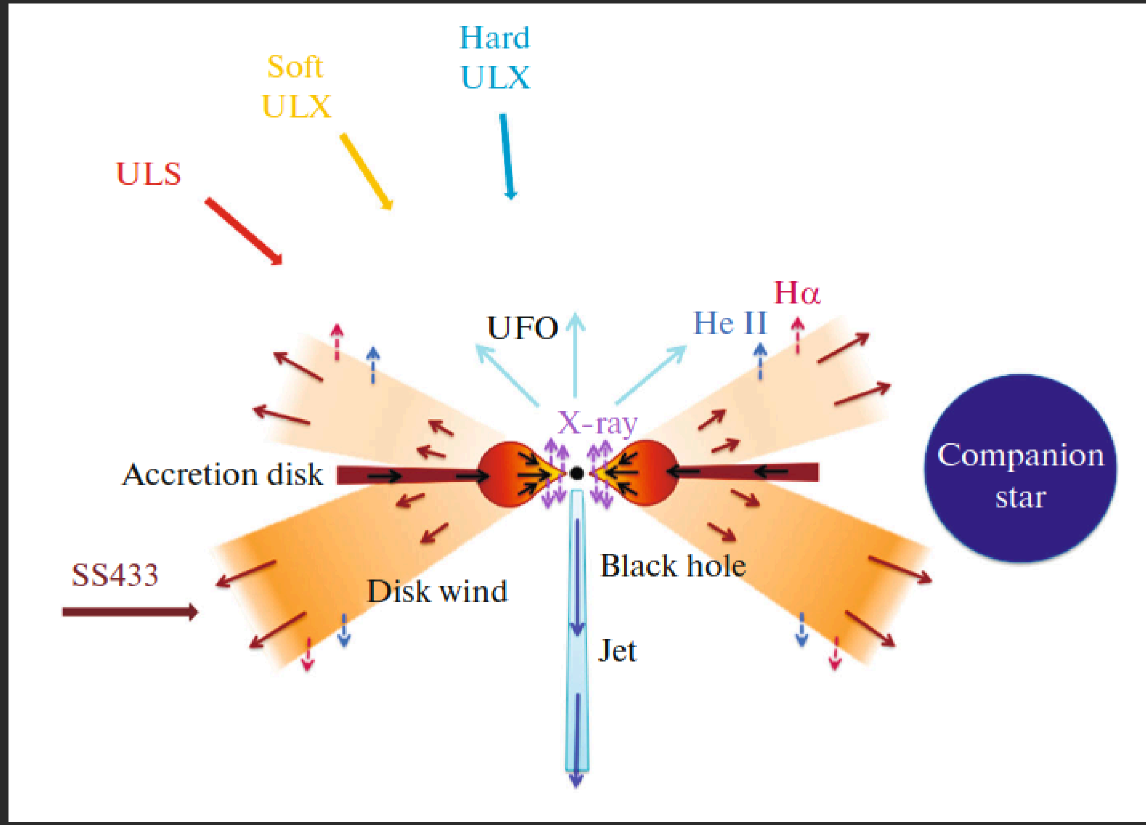

Fabrika et al. 2021

ULXs show several different X-ray spectral states classified according to “standard disk” (soft) and “comptonization” (hard) relative dominance.

ULXs can transition between them, and are consistent with a geometrical perspective of the observer relative to the accretion disk and funnel.

Precession affects accretion disk angle, while changes in accretion rates can affect the funnel opening angle (expected variability).

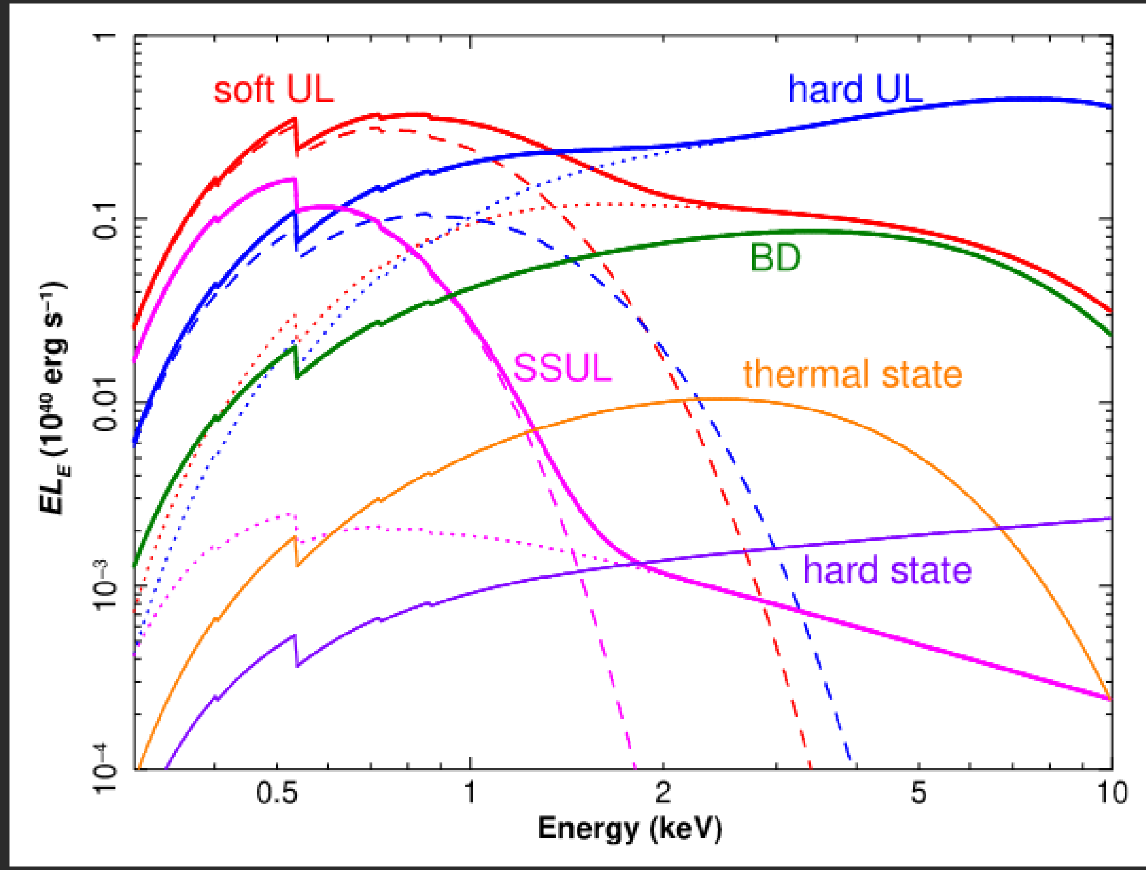

II. Timing properties of NGC 4190 ULX1

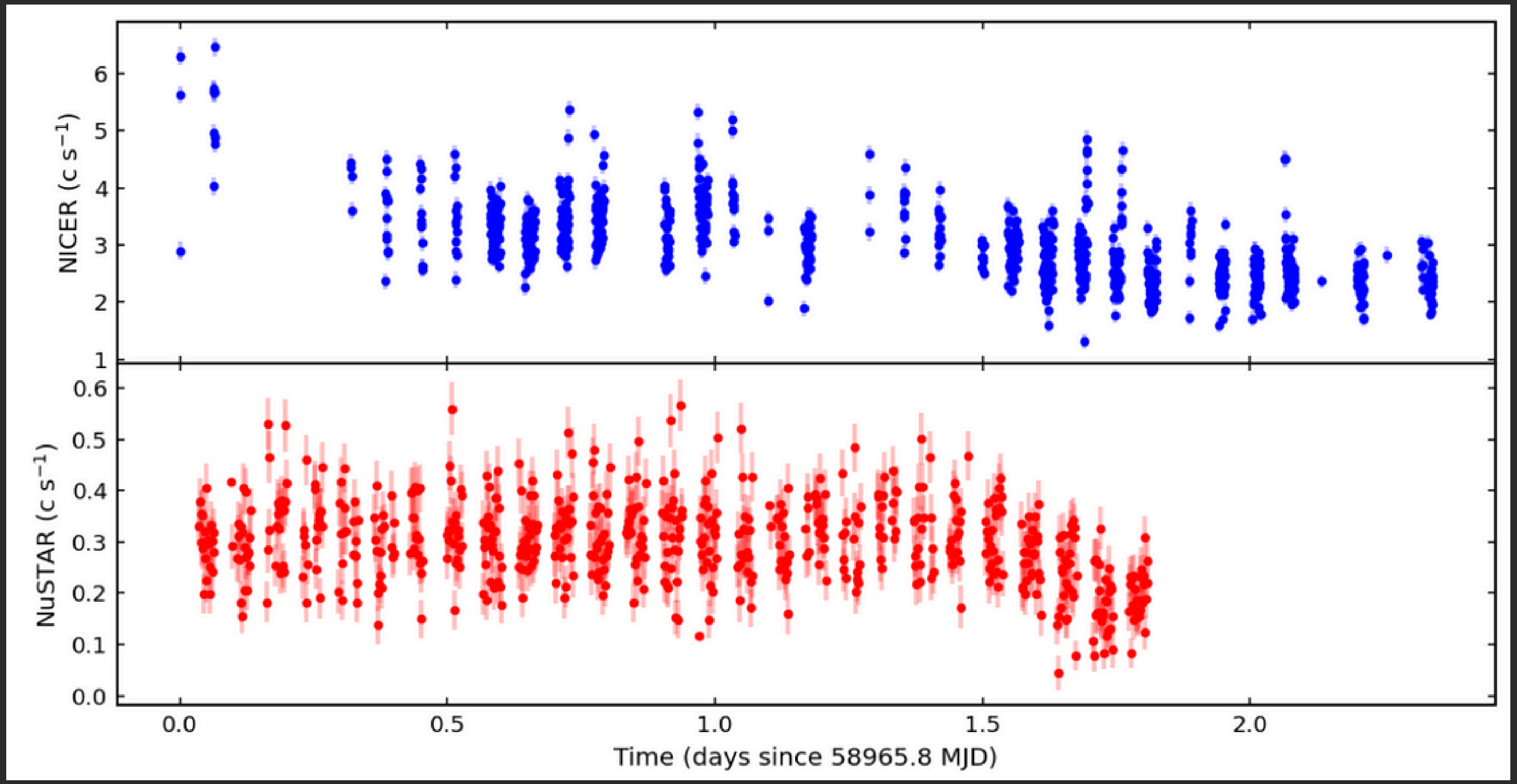

NICER (0.3 - 12 keV) + **NuSTAR** (3 - 79 keV)
~50hr exposure between April 26-28, 2020

No flaring activity

Slight count rate (CR) decrease associated to changes in local absorption (CR constant above 10 keV)

II. Timing properties of NGC 4190 ULX1

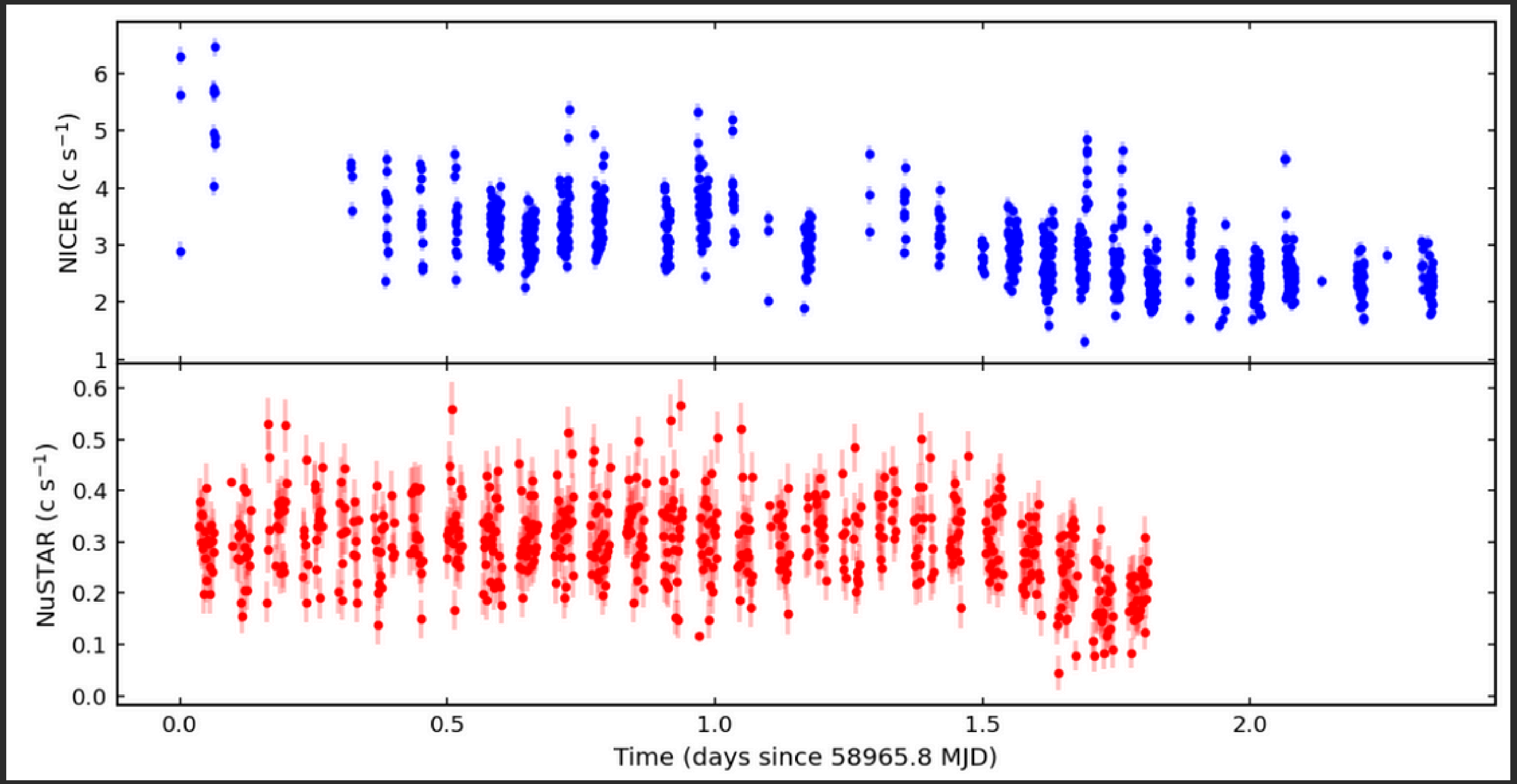

NICER (0.3 - 12 keV) + **NuSTAR** (3 - 79 keV)
~50hr exposure between April 26-28, 2020

No flaring activity

Slight count rate (CR) decrease associated to changes in local absorption (CR constant above 10 keV)

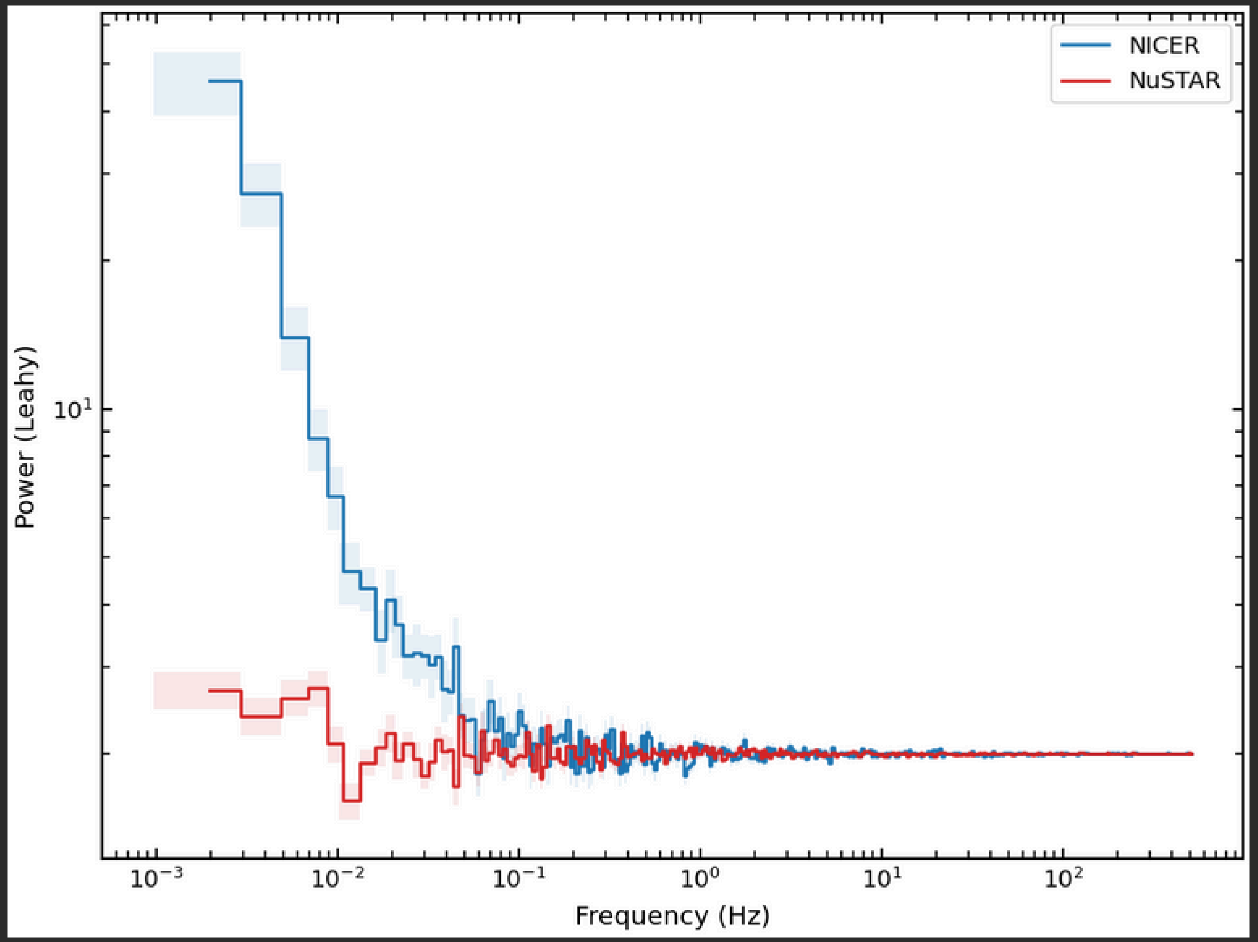

No evidence of pulsations between **0.01 - 10 Hz** using acceleration algorithms (**HENDRICS**).

Pulsed fraction **upper limits:**
NICER : 7%
NuSTAR: 18%

III. Spectral properties of NGC 4190 ULX1

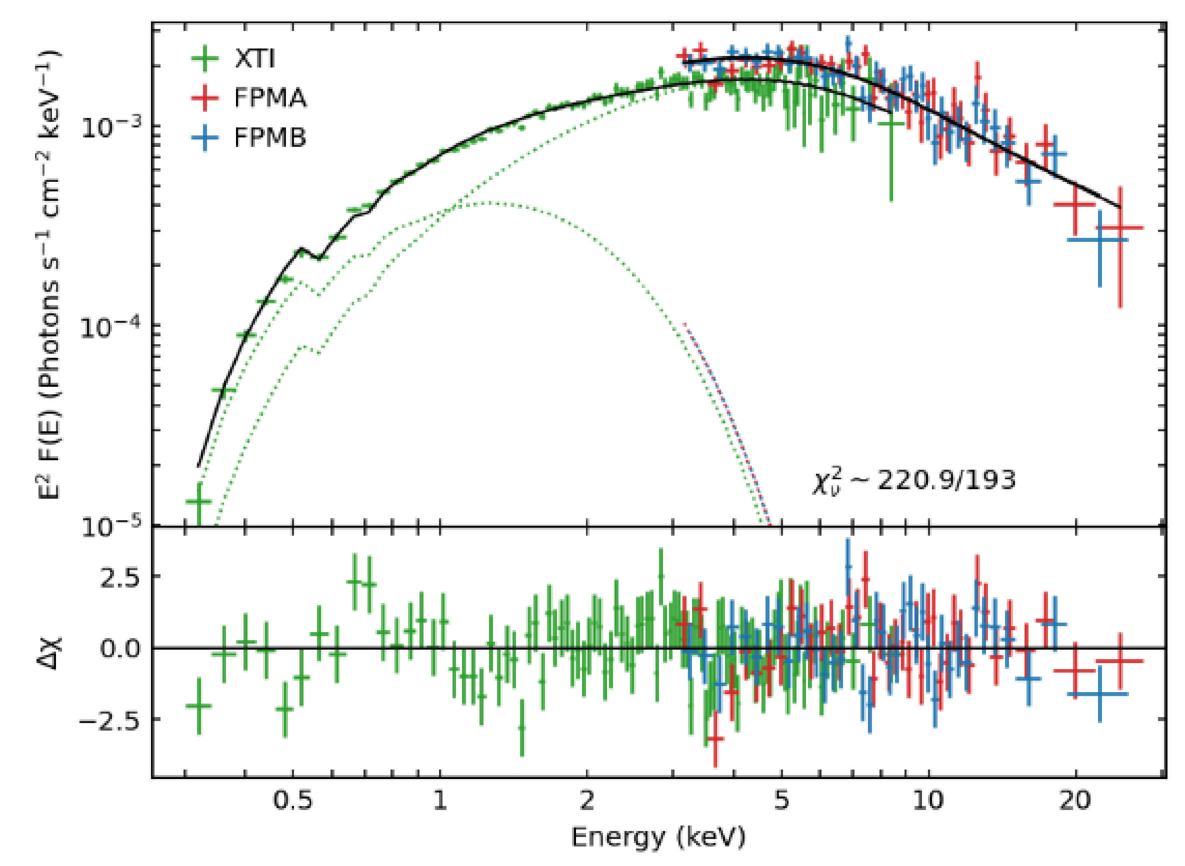

BH scenario: DISKBB + SIMPL*DISKPBB

DISKBB : outer accretion disk (geom. thin, optically thick, **p=0.75**)
DISKPBB: inner accretion disk (deviates from thin disk, **p** free)
(Temperature radial profile proportional to r^{-p})
SIMPL: Comptonization from hot electron plasma in the funnel.

kT ~ 0.4 keV   kT ~ 1.2 keV   p>0.7

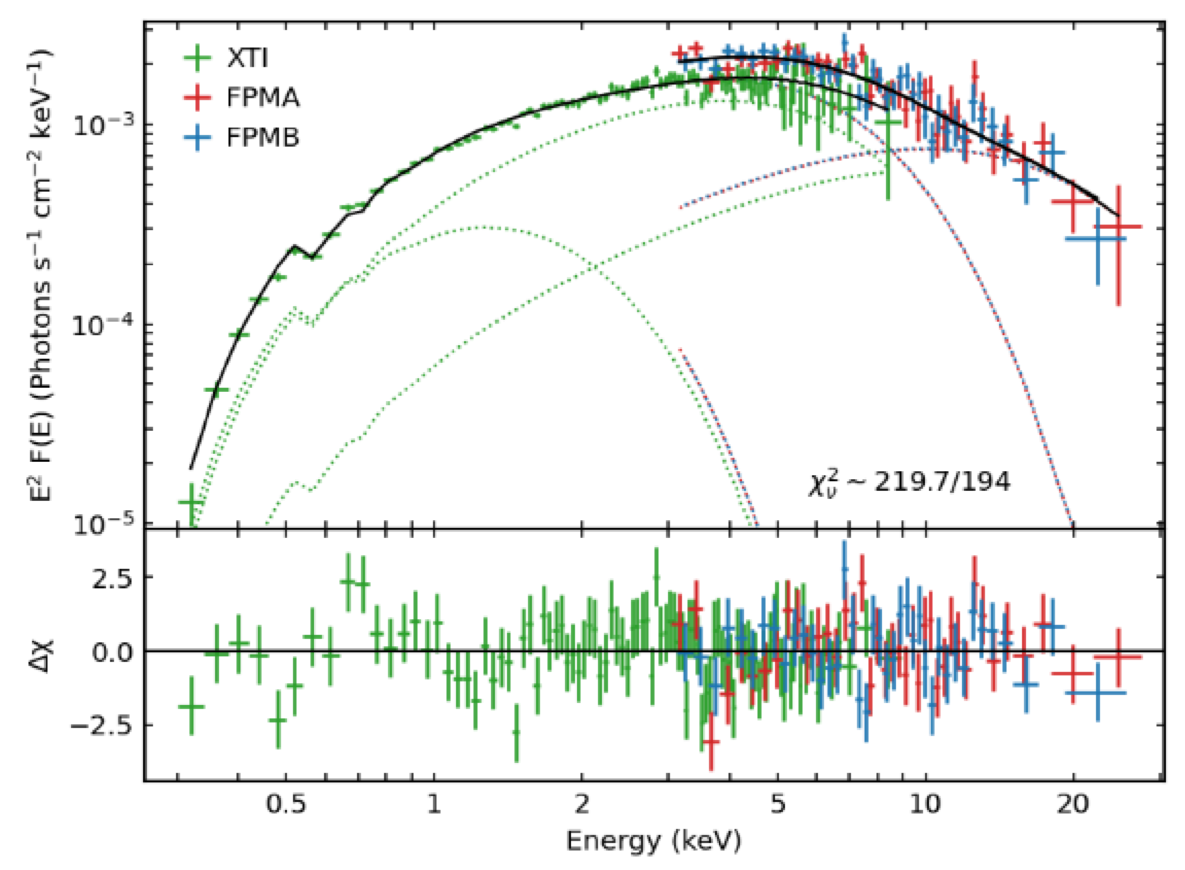

NS scenario (PULX): DISKBB + DISKPBB + CUTOFFPL

DISKBB + DISKPBB : accretion flow in the disk and magnetosphere.
CUTOFFPL: radiation from matter in the accretion column.
We took average values of Sp.Index=0.59 and cutoff energy (7.9 keV)

kT ~ 0.4 keV   kT ~ 1.7 keV   p>0.7

Luminosity (0.3 - 30 keV) ~ 7.6*10**39 erg/s @ 2.9 Mpc
(Soft ultraluminous state)

IV. NGC 4190 ULX1 compared to PULXs

No pulsations detected between 0.01 - 10 Hz.

Luminosity vs. Hardness places NGC 4190 ULX1 in between pulsating and non pulsating systems.

Cutoffpl flux / Total flux ~ 28%
(PULX usually closer to 50%)

PULX nature of NGC 4190 could not be confirmed.

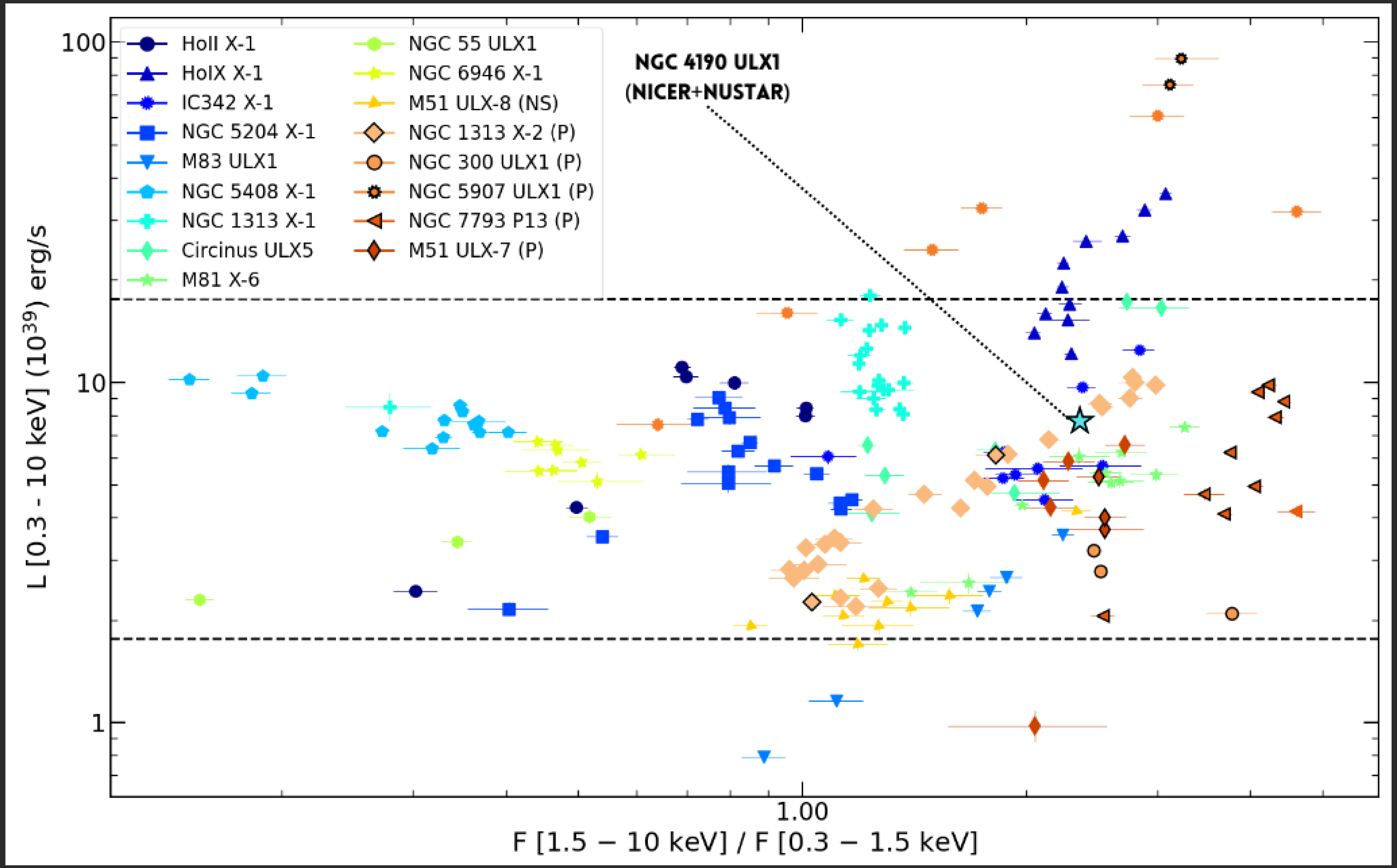

Adapted from Gúrpide et al. 2021

V. Testing the L-T relationship

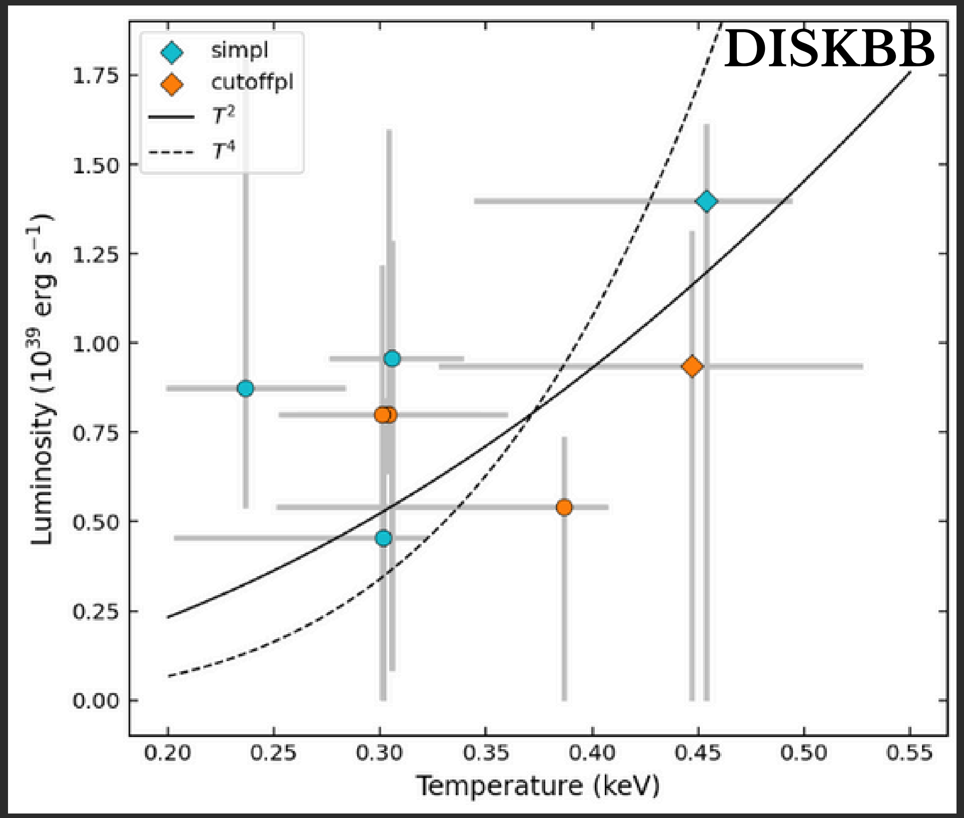

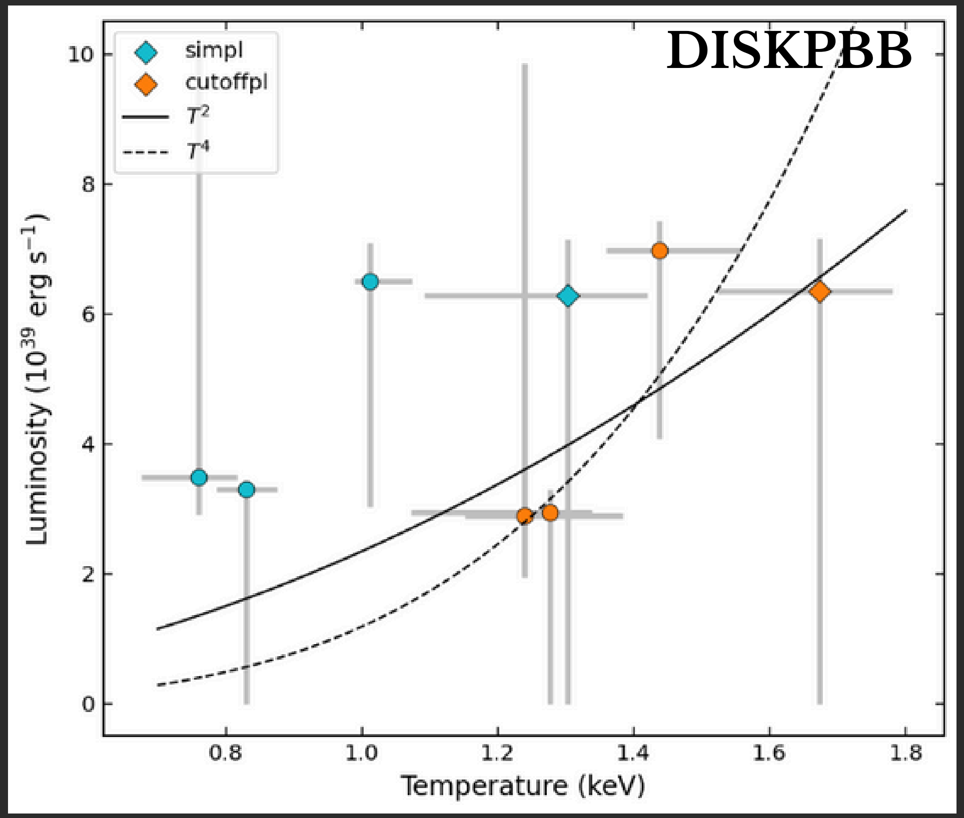

We reprocessed archival XMM-Newton observations

0.3-30 keV luminosities vs BB temperature

Both disk components show a **favoring** case to
T2** (thick disk, **advection** dominated)
with respect to
T4** (thin disk, sub Eddington accretion rate)

Motivated us to apply a more
physically driven model
(Abaroa et al., 2023)

VI. Supercritical disk wind model

10 solar mass BH accreting from an massive companion (B2V) at 10 times the Eddington rate.

Two disk regions: **outer** (optically thick, geom. thin) **inner** (geom. thick, radiation dominated with advection)

Critical radius at which radiation pressure dominates over gravitational atraction, creating **opaque wind outflows**. Funnel created by angular momentum conservation.

X-ray radiation escapes only through the funnel (inner disk). The rest of disk X-ray radiation is absorbed or downscattered.

Geometrical beaming increases the apparent luminosity with beaming factor b=0.73 for NGC 4190 ULX1

$$L_{\rm iso} \approx L_{\rm Edd}\left[1 + \frac{\ln \dot{m}}{b}\right]$$

Hard X-ray emission coming from a hot plasma in the funnel above the BH : relativistic non thermal electrons Comptonize softer photons from the disk.

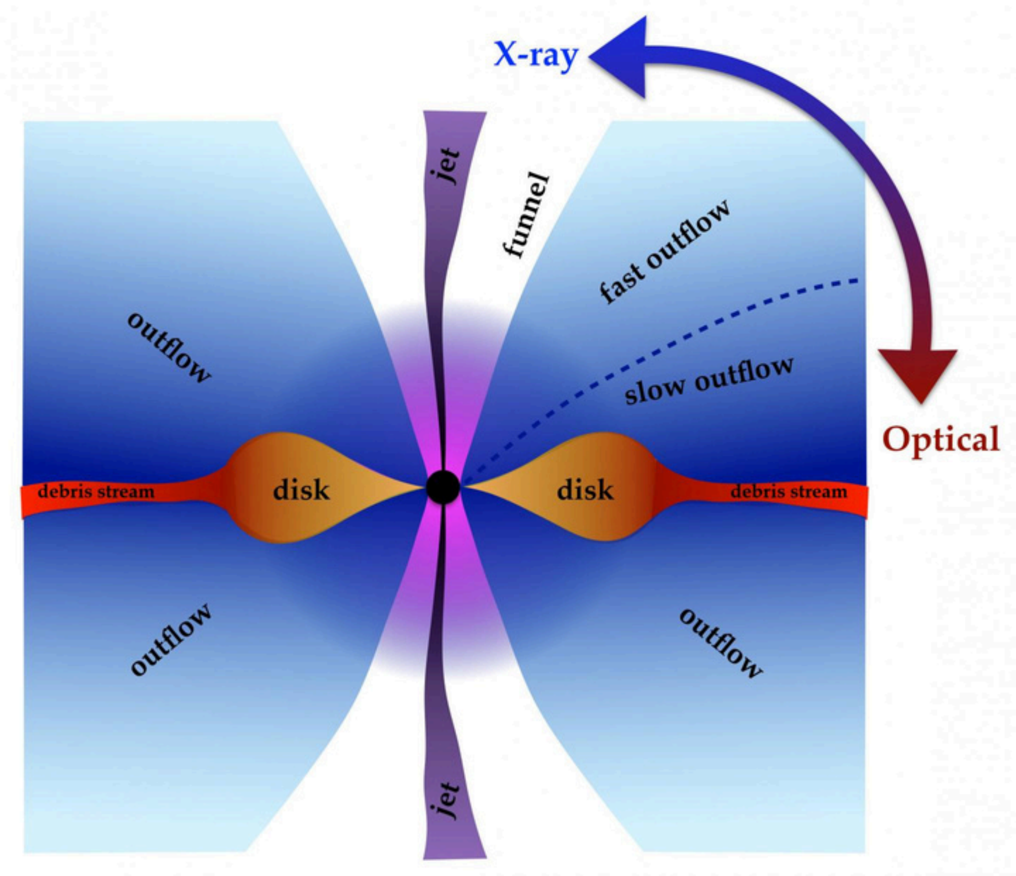

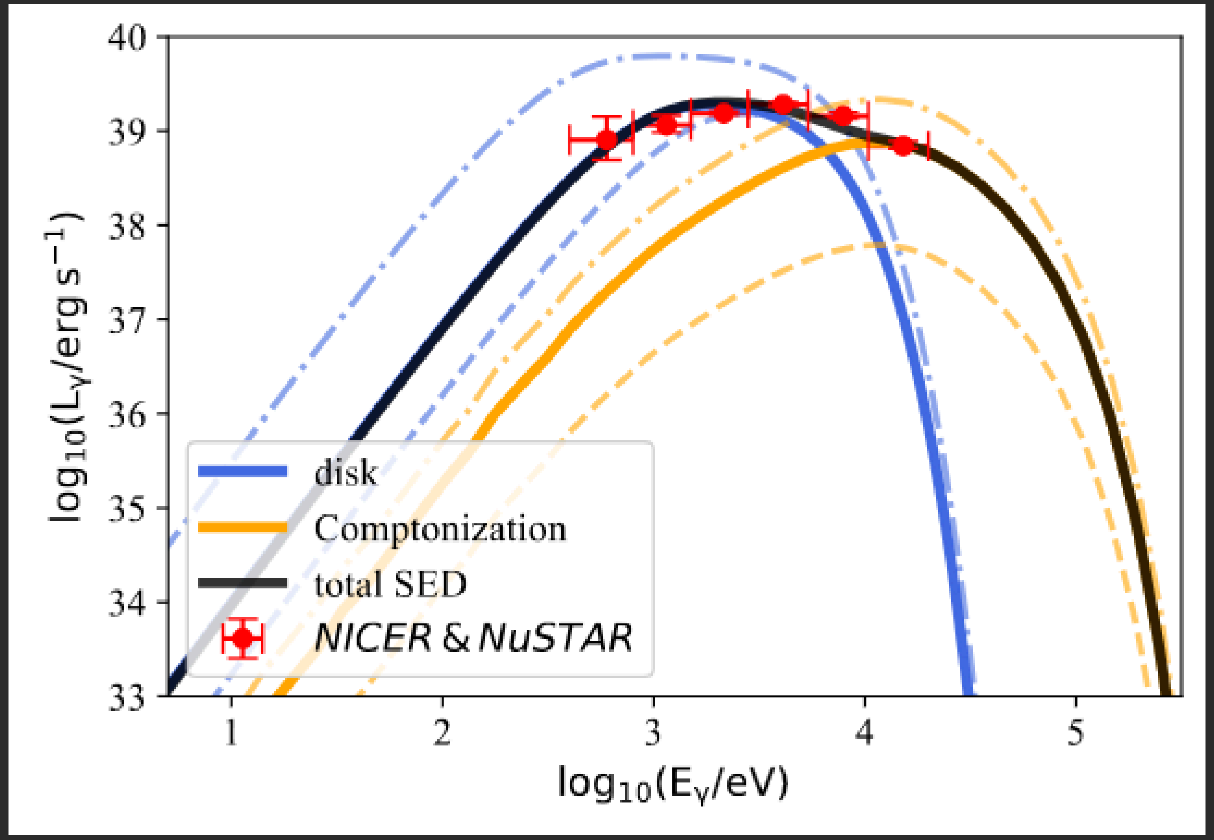

VII. Main take aways

- NGC 4190 ULX1 observed by NICER+NuSTAR during a quiescent state.
- No pulsations were detected, but hard flux ratios do not discard NS nature.
- Spectral show typical SUL state behaviour (two thermal components plus comptonization tail)
- The tail is consistent with a funnel above de BH, with hot electrons capable of upscattering softer photons from the inner disk region.
- We were able to succesfully model the NICER+NuSTAR data assuming a 10 solar mass BH accreting at a rate of ~10 times the Eddington rate.

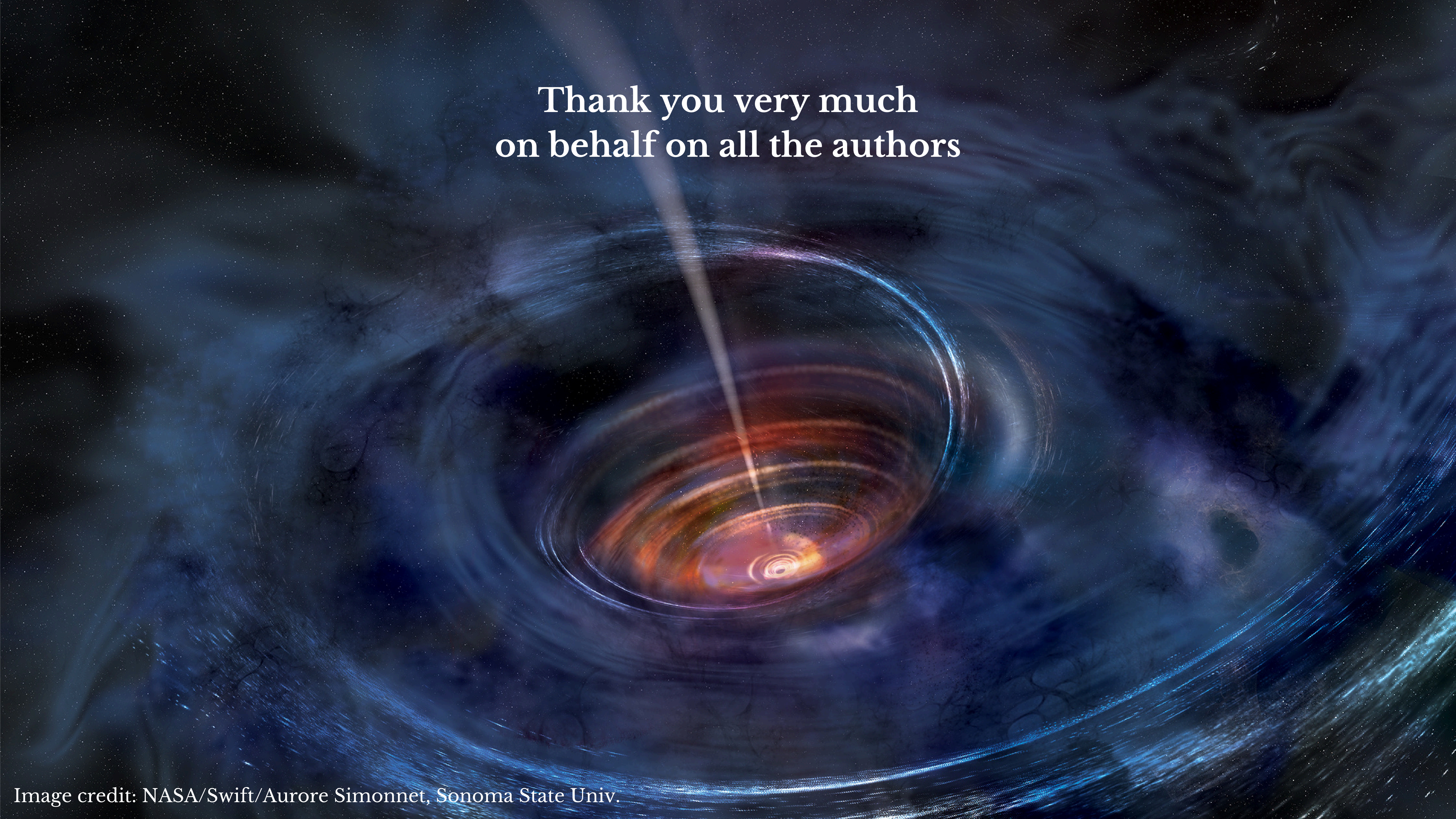

Image credit: NASA/Swift/Aurore Simonnet, Sonoma State Univ.

Appendix: NICER+NuSTAR best fit parameters

Component	Parameter	Model	
		SIMPL	CUTOFFPL
CONS	$C_{\mathrm{A/XTI}}$	1.26 ± 0.06	1.26 ± 0.06
	$C_{\mathrm{B/XTI}}$	1.29 ± 0.06	1.28 ± 0.06
TBABS	N_{H} (10^{22} cm^{-2})	$0.09^{+0.02}_{-0.01}$	0.09 ± 0.02
DISKBB	kT_{in} (keV)	0.4 ± 0.1	0.4 ± 0.1
CUTOFFPL	Γ	–	$0.59^{(\dagger)}$
	E_{fold} (keV)	–	$7.1^{(\dagger)}$
SIMPL	Γ	3.4 ± 0.3	–
	CF	$0.9^{+0.1}_{-0.4}$	–
DISKPBB	kT (keV)	$1.2^{+0.3}_{-0.1}$	$1.7^{+0.2}_{-0.1}$
	p	$0.8^{+0.2}_{-0.1}$	$0.7^{+0.2}_{-0.1}$
Luminosity	10^{39} erg s^{-1}	7.6 ± 0.2	
χ^2/d.o.f.		220.9/193	219.7/194

Appendix: wind model parameters

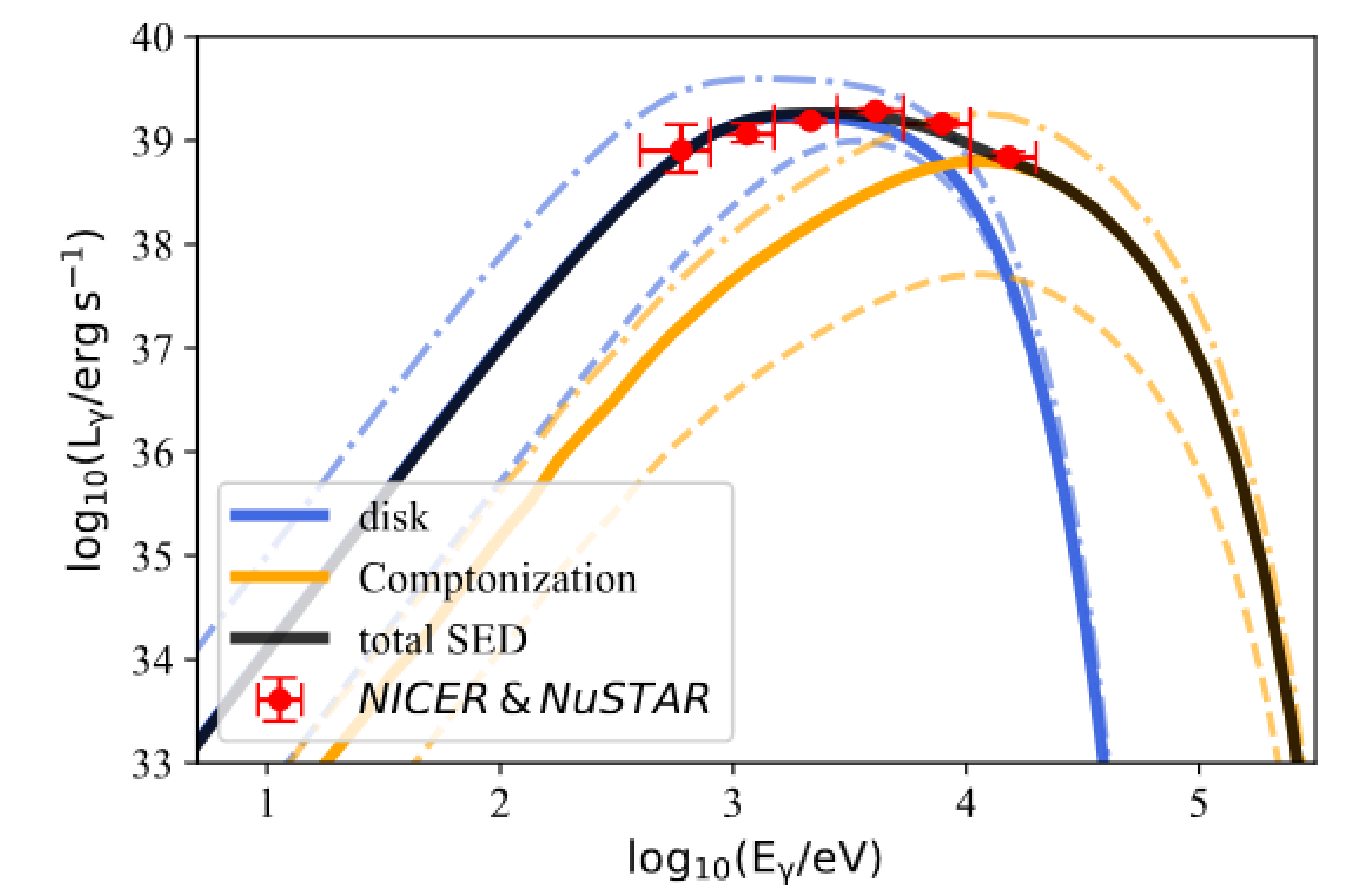

Parameter	Symbol	Value	Units
Black hole mass [(1)]	$M_{\rm BH}$	10	$M_\odot$
Gravitational radius [(2)]	$r_{\rm g}$	1.48×10^6	cm
Critical radius [(2)]	$r_{\rm crit}$	3.5×10^9	cm
Eddington accretion rate [(2)]	$\dot{M}_{\rm Edd}$	2.2×10^{-7}	$M_\odot\,{\rm yr}^{-1}$
Mass accretion rate [(1)]	$\dot{M}_{\rm input}$	2.2×10^{-6}	$M_\odot\,{\rm yr}^{-1}$
Hot gas Lorentz factor [(2)]	$\gamma_{\rm dw}$	1.25	
Geometric beaming factor [(2)]	b	0.73	
Hadron-to-lepton ratio [(1)]	a	0.01	
Kinetic power of electrons [(2)]	$L_{\rm K}^{\rm dw}$	2.2×10^{39}	${\rm erg\,s^{-1}}$
Content of relativistic particles [(1)]	$q_{\rm rel}$	0.15	
Injection spectral index [(1)]	p	2	
Viewing angle [(1)]	i	≈ 0	deg

Notes. We indicate the parameters that we have assumed with superscript (1) and those that we have derived with (2).

Appendix: XMM-Newton best fit parameters

Component	Parameter	Observation 0654650101 SIMPL	0654650101 CUTOFFPL	0654650201 SIMPL	0654650201 CUTOFFPL	0654650301 SIMPL	0654650301 CUTOFFPL
CONS	C_{MOS1}	0.99 ± 0.03	0.99 ± 0.03	$1.09^{+0.02}_{-0.03}$	$1.08^{+0.02}_{-0.03}$	1.01 ± 0.02	$1.01^{+0.03}_{-0.02}$
	C_{MOS2}	0.95 ± 0.03	0.94 ± 0.03	$1.04^{+0.03}_{-0.02}$	$1.04^{+0.02}_{-0.03}$	1.03 ± 0.02	1.03 ± 0.02
TBABS	N_H (10^{22} cm^{-2})	$0.06^{+0.05}_{-0.04}$	$0.03^{+0.04}_{-0.02}$	$0.13^{+0.04}_{-0.03}$	0.1 ± 0.03	0.09 ± 0.03	$0.1^{+0.02}_{-0.03}$
DISKBB	kT_{in} (keV)	0.3 ± 0.1	0.4 ± 0.1	0.24 ± 0.03	$0.29^{+0.05}_{-0.04}$	$0.3^{+0.06}_{-0.05}$	$0.3^{+0.08}_{-0.05}$
CUTOFFPL	Γ	–	$0.59^{\dagger}$	–	$0.59^{\dagger}$	–	$0.59^{\dagger}$
	E_{fold} (keV)	–	$7.1^{\dagger}$	–	$7.1^{\dagger}$	–	$7.1^{\dagger}$
SIMPL	Γ	$3.4^{\dagger}$	–	$3.4^{\dagger}$	–	$3.4^{\dagger}$	–
	CF	$0.9^{\dagger}$	–	$0.9^{\dagger}$	–	$0.9^{\dagger}$	–
DISKPBB	kT (keV)	$0.84^{+0.1}_{-0.06}$	$1.3^{+0.1}_{-0.2}$	0.76 ± 0.03	$1.23^{+0.09}_{-0.06}$	$1^{+0.1}_{-0.05}$	1.4 ± 0.2
	p	$0.9^{+0.1}_{-0.2}$	$0.9^{+0.1}_{-0.2}$	0.95 ± 0.05	$0.95^{+0.05}_{-0.2}$	0.9 ± 0.1	$0.8^{+0.2}_{-0.1}$
Luminosity	10^{39} erg s^{-1}	3.7 ± 0.4		4.3 ± 0.5		7.5 ± 0.7	
χ^2/dof		299.3/232	297.8/231	244.1/232	222.0/231	263.7/274	264.3/273